Climate Dynamics (2018) 51:2543–2558
https://doi.org/10.1007/s00382-017-4027-9

Effects of intraseasonal oscillation on South China Sea summer monsoon onset

Hui Wang[1] · **Fei Liu**[1] · **Bin Wang**[2] · **Tim Li**[2]

Received: 2 September 2017 / Accepted: 29 November 2017 / Published online: 9 December 2017

Abstract
Understanding of South China Sea (SCS) summer monsoon (SCSSM) onset response to tropical intraseasonal oscillation (ISO) is critical for extended-range prediction of SCSSM onset. In this study, we investigate the effect of ISO on SCSSM onset for the period of 1980–2013. The 34 onset cases are classified into three groups, early onsets around May 6th, normal onsets around May 21st and late onsets around June 8th, and the late onsets are even later than the Indian monsoon onsets. Before each onset, the SCS experiences a dry ISO phase to precondition the convective energy due to the easterly wind anomalies of the wet ISO phase over the tropical Indian Ocean for the group of early onsets, over the southern Bay of Bengal monsoon region for the group of normal onsets and over the southern Indian monsoon region for the group of late onsets. After each onset, the SCSSM is supported by the westerly wind anomalies of the dry ISO phase over these associated regions. Each early SCSSM onset is triggered by the northwestward propagating Rossby wave of the wet ISO in the western Pacific which comes from the Indian Ocean. For each normal (late) onset, the SCSSM is triggered by synoptic-scale low-level westerlies in conjunction with seasonal low-level westerlies when the wet ISO moves to the northern Bay of Bengal region (Indian monsoon region), since this convection to the north of 10°N cannot excite the easterly wind anomalies associated with Kelvin wave responses over the SCS to suppress the convection. The mechanisms explaining the mean state-controlled ISO-SCSSM onset relationship are also discussed.

Keywords South China Sea summer monsoon · Monsoon onset · Intraseasonal oscillation · Bay of Bengal summer monsoon · Indian summer monsoon

1 Introduction

The South China Sea (SCS) summer monsoon (SCSSM) is an important component of the East Asian summer monsoon system, whose onset signifies the commencement of the East Asian summer monsoon and the beginning of the rainy season (Wang 2002; Wang et al. 2004; Ding and He 2006; Kueh and Lin 2009). The SCSSM onset is usually characterized by the reversal of low-level zonal wind from easterlies to westerlies over the key region of 110–120°E, 5–15°N and a sharp increase in rainfall over the SCS between 10°N and 20°N (Wu and Wang 2000, 2001; Wu 2002, 2010; Wang et al. 2004; Shao et al. 2014). The SCSSM is closely related to other Asian monsoon systems since the SCS is geographically located at the joint region of the East Asian monsoon, the South Asian monsoon, the western North Pacific (WNP) monsoon, and the Australian monsoon (Murakami and Matsumoto 1994; Wang et al. 2009a, b; Zhou et al. 2011; Kajikawa and Wang 2012). The onset and development of the SCSSM not only have important influences on the summer precipitation in eastern China, which is closely related to climate disasters such as floods and droughts, but also affect global climate through teleconnections, such as the Pacific-Japan Pattern and the Rossby wave trains from the Philippines to North America (Nitta 1987; Ding 1992; Huang and Sun 1992). Therefore, the study of SCSSM, especially that of SCSSM onset prediction, is of great importance.

Extended-range prediction of the SCSSM onset is important for the society of all Asian countries. This requires a

✉ Fei Liu
liuf@nuist.edu.cn

[1] Earth System Modeling Center and Climate Dynamics Research Center, Nanjing University of Information Science and Technology, Nanjing 210044, China

[2] Department of Atmospheric Sciences and Atmosphere-Ocean Research Center, University of Hawaii at Manoa, Honolulu, HI 96822, USA

good understanding of the relationship between SCSSM onset and tropical intraseasonal oscillation (ISO). The ISO is the dominant intraseasonal variability in the tropics, which is identified by the boreal winter Madden-Julian oscillation (MJO; Madden and Julian 1971, 1972) and by the boreal summer intraseasonal oscillation (BSISO; Wang and Xie 1996). The former is characterized by the eastward propagation along the equator, while the latter, by the northeastward propagation over the Indian Ocean and northwestward propagation over the western Pacific. The ISO provides a predictability source for extended-range weather forecasts, and helps close the gap between traditional weather prediction and modern-day climate prediction (Zhang 2013). The ISO during the boreal summer has been well studied (Kajikawa and Yasunari 2005; Yang et al. 2008; Kajikawa et al. 2009; Wang et al. 2009a, b; Liu et al. 2015a, b, 2016b; Wu and Cao 2017). These studies, however, all focused on the ISO after the monsoon onset. The ISO evolution before the monsoon onset was less studied.

Generally, the establishment of the SCSSM has been found to be triggered by low-frequency oscillation after the seasonal change (Murakami et al. 1986), and the onset is consistent with the phase transition from dry to wet of the SCS ISO (Wang and Xu 1997; Shao et al. 2014). The timing of the SCSSM onset is primarily determined by the phase-locking of northwestward propagating 10–20-day and northeastward propagating 30–60-day modes (Mao and Chan 2005; Zhou and Chan 2005). For example, the SCSSM onset in 1998 was found to be preceded by the development of an eastward-propagating MJO in the Indian Ocean, and the subsequent emanation of a convectively coupled Kelvin wave into the Pacific (Straub et al. 2006). A frontal cyclone, which is associated with 12–24-day ISO initiated from northeastern China can move equatorward into the SCS and affect the monsoon onset there (Chen and Chen 1995; Chan et al. 2000; Ding and Liu 2001; Tong et al. 2008). It is found that most of SCSSM onsets occur in phases 2–4 when the BSISO2-related convection is in the Philippine Sea and the SCS (Lee et al. 2013). BSISO2 represents the northwestward propagation of the BSISO, comprised of the 3rd and 4th multivariate empirical orthogonal function (MV-EOF) modes for the boreal summer OLR and 850-hPa zonal wind. The ISO activity originating from the equatorial western Pacific also can move northward to affect the SCSSM onset (Wu 2010). These studies, however, only focused on climatological relationships between the ISO and SCSSM onset. It is not clear how interannual and interdecadal variabilities modulate this relationship.

Many previous studies have indicated that the SCSSM onset exhibits significant interdecadal and interannual variability which are associated with many factors including sea surface temperature anomalies (SSTa) and land surface temperature anomalies. For example, a warm ENSO event during the previous winter (Zhou and Chan 2007), warm SSTa in the tropical Indian Ocean during the previous winter (Yuan et al. 2008), or cold SSTa over the equatorial western Pacific during the spring (Wu and Wang 2000; Yuan and Chen 2012; Liang et al. 2013) all can delay the onset by inducing an anomalous reversed Walker circulation over the tropical Indo-Pacific Ocean and hence suppressing the convection over the western Pacific. The situation is opposite for the early onset year. In addition, the SCSSM onset can be delayed by negative surface air temperature anomalies over land in the central Asian continent (Luo et al. 2016), warm spring SSTa in the southern Indian Ocean (Liu et al. 2016a), and delay of thermal contrast reversal between Indo-China Peninsula and SCS (Liu et al. 2010). Thus, it is necessary to study how these interannual-to-decadal variabilities modulate the ISO-SCSSM onset relationship.

A late (early) SCSSM onset was found to be accompanied by active (suppressed) 10–25-day ISO, while the onset day was negatively correlated with the 30–60-day ISO activity (Kajikawa and Yasunari 2005). After examining the three types of SCSSM onset, i.e., the early, normal and late onsets, almost all the SCSSM onsets have been found to occur during the so-called developing phase of ISO (Shao et al. 2014). The monsoon onset often occurs during the active convective and developing phase of ISO in the early- and normal-onset years, but it occurs during the inactive convective and developing phase of ISO in the late-onset years. In these studies, the authors only focused on the local SCS ISO. Evolutions of the ISO related to these SCSSM onsets, however were not considered; thus, it is not clear how the ISO prevailing over the Indo-western Pacific region affects the three types of SCSSM onsets. In this study, we aim to analyze the evolution of the ISO related to each of these three types of SCSSM onsets, as well as its relation with other monsoon systems, such as the Bay of Bengal summer monsoon and the Indian summer monsoon. The mechanisms behind these three types of ISO-SCSSM onset relationships are also discussed.

The organization of the paper is as follows. In Sect. 2, we introduce the dataset and methods used in present study. In Sect. 3, we calculate the dates of SCSSM onsets and classify them into three types, i.e., the early onset, the normal onset and the late onset. In Sect. 4, the relationships between the local SCS ISO and these three types of SCSSM onsets are discussed. In Sect. 5, we analyze the characteristics of ISO, which affect these different SCSSM onsets. The underlying mechanisms of ISO-controlled SCSSM onsets are presented in Sect. 6. We conclude the study in Sect. 7.

2 Data and methods

The data used in this study include daily-mean wind, air temperature, specific humidity and relative humidity from 1000 to 300 hPa, which are obtained from the National Centers for Environmental Prediction–the National Center for Atmospheric Research (NCEP-NCAR) reanalysis project (Kalnay et al. 1996), and the daily sea surface temperature (SST) from the European Centre for Medium-Range Weather Forecasts (ECMWF) reanalysis-interim (ERA-interim) data (Dee et al. 2011). In addition, the daily-mean Advanced Very High Resolution Radiometer (AVHRR) interpolated outgoing long-wave radiation (OLR) data from the National Oceanic and Atmospheric Administration (NOAA) satellite are used as an indicator of convection activity (Liebmann 1996). The negative OLR anomaly represents active convection and positive precipitation anomaly. The horizontal resolution of all datasets is 2.5° × 2.5°, and the temporal coverage is from 1980 to 2013.

A 12–80-day butterworth bandpass filter is applied to isolate the intraseasonal anomalies, and an 81-day Gaussian lowpass filter, to isolate the low-frequency anomalies. In addition, the synoptic anomalies are calculated by using the original data minus the 11-day lowpass-filtered anomalies.

Background atmospheric convective instability is one of the factors that can affect the development of the ISO. A positive convective instability implies that the atmosphere is potentially unstable, and it favors the development of convection. The convective instability parameter is defined as the difference of equivalent potential temperature (θe) between the lower and middle troposphere (Zhang et al. 2004; Ding and He 2006; Li et al. 2012), i.e., $\Delta\theta e = \theta e|_{1000-700\text{hPa}} - \theta e|_{600-300\text{hPa}}$.

3 Definition of SCSSM onset date

There are many definitions for the SCSSM onset date, which capture different characteristics of the SCSSM onset by using the associated variables including the low-level zonal wind (Wang et al. 2004), the temperature of black body on the top of cloud (He et al. 2006), the equivalent potential temperature (Gao et al. 2001), the meridional temperature gradient (Mao et al. 2004; Liu et al. 2016a), or combined measures of convection and low-level wind (Xie et al. 1998; Kueh and Lin 2009; Shao et al. 2014). In this work, we use the definition of Wang et al. (2004), namely, the low-level zonal wind that is coupled to the convection. Following previous studies (Wang et al. 2004; Kajikawa and Wang 2012), the SCSSM onset date of each year is determined by using the daily-mean SCSSM wind index, i.e., the box (110–120°E, 5–15°N) averaged 850-hPa zonal wind. The onset date of the SCSSM is then defined by the first day after April 25th, which satisfies the following three criteria: (1) on the onset day and during the five days after the onset day, the averaged SCSSM index must be greater than zero, meaning that the westerly is steadily established; (2) in the subsequent 20 days, which includes the onset pentad, the SCSSM index must be positive for at least 15 days and (3) the cumulative 20-day-mean SCSSM index must be greater than 1 m s^{-1}, for a persistent seasonal transition.

Based on the above definition, Fig. 1 shows the time series of monsoon onset dates of the 34 years from 1980 to 2013. We can see that the climatological-mean onset date is May 22nd, and that the onset date has a significant decadal shift. Compared to that before 1994, the onset of the SCSSM tended to be earlier in the recent decades, as shown by many studies (Kajikawa and Wang 2012; Yuan and Chen 2012; Liu et al. 2016a). In addition, the interannual variation of the SCSSM onset is also significant, with the earliest onset in late-April and the latest in mid-June. In this paper, we define the SCSSM onset as an early onset when the onset date is less than −0.75 standard deviation, and a late onset, larger than 0.75 standard deviation. Following this criterion, there were nine early onset years including 1986, 1994, 1996, 2000, 2001, 2004, 2008, 2009, and 2012. The 10 years of 1980, 1983, 1984, 1987, 1989, 1991, 1992, 1993, 2006, and 2013 are identified as the late onset years. The remaining 15 years are the normal onset years. Note that most (8 out of 10) of late onset years occurred before 1994 while eight out of nine early onset years occurred after 1994. The averaged onset date for these nine early onsets is May 6th, and that for the 10 late onsets is June 8th. The difference between these

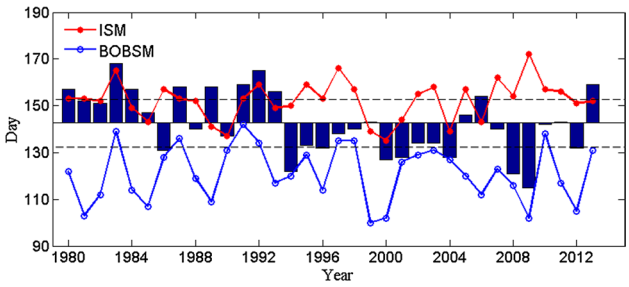

Fig. 1 Different Asian summer monsoon onset dates. Time series of the onset dates of the South China Sea summer monsoon (SCSSM, bars), Indian summer monsoon (ISM, red dots) and Bay of Bengal summer monsoon (BOBSM, blue circles) defined based on the 850-hPa zonal wind for the period of 1980–2013. All dates are Julian dates in the calendar year (e.g., day 121 = May 1st, etc.). Dashed lines denote the 0.75 standard deviations of the time series of SCSSM onset dates

late and early onsets is more than a month, and is statistically significant. The averaged date for the normal onsets is May 21st.

In Fig. 1, the Bay of Bengal summer monsoon onset and the Indian summer monsoon onset are also shown as references. The Bay of Bengal summer monsoon onset date for each individual year is defined as the day when the 850-hPa zonal wind over the eastern Bay of Bengal (90–100°E, 5–15°N) changes from negative to positive and remains positive for more than 10 days (Mao and Wu 2006). The Indian summer monsoon onset is defined as the first day when the 850-hPa zonal wind averaged over the southern Arabian Sea region (40–80°E, 5–15°N) continuously exceeds 6.2 m s^{-1} for more than 7 days (including the onset day) (Wang et al. 2009a, b). Consistent with previous works (Liu et al. 2002, 2014; Wang and LinHo 2002; He et al. 2006), there are three consecutive stages for the onset of these different Asian summer monsoon systems. The Bay of Bengal summer monsoon onset occurs first around May 1st, then the SCSSM, near May 22st and the Indian summer monsoon, near June 1st. Some studies indicated the role of Bay of Bengal summer monsoon convection in the SCSSM onset (Liu et al. 2002), while few studies investigated the effect of Indian summer monsoon on the SCSSM. In this study, the relationship among the SCSSM, Bay of Bengal summer monsoon and Indian summer monsoon onsets associated with different ISO evolutions is discussed.

The climatological onset date based on the zonal wind, i.e., May 22nd, is about 1 week later than that determined by using precipitation in the work of Wu and Wang (2000). One reason may be attributed to different thresholds used to define the onset. In Wu and Wang (2000), a weak threshold of 240 w m^{-2} was used. The onset date defined by the zonal wind (Wang et al. 2004; Kajikawa and Wang 2012), on the other hand, coincides with the onset date defined by a strong threshold of 220 w m^{-2} (Kueh and Lin 2009). Certainly, there are other reasons for these different onset dates, and they will be investigated in the future.

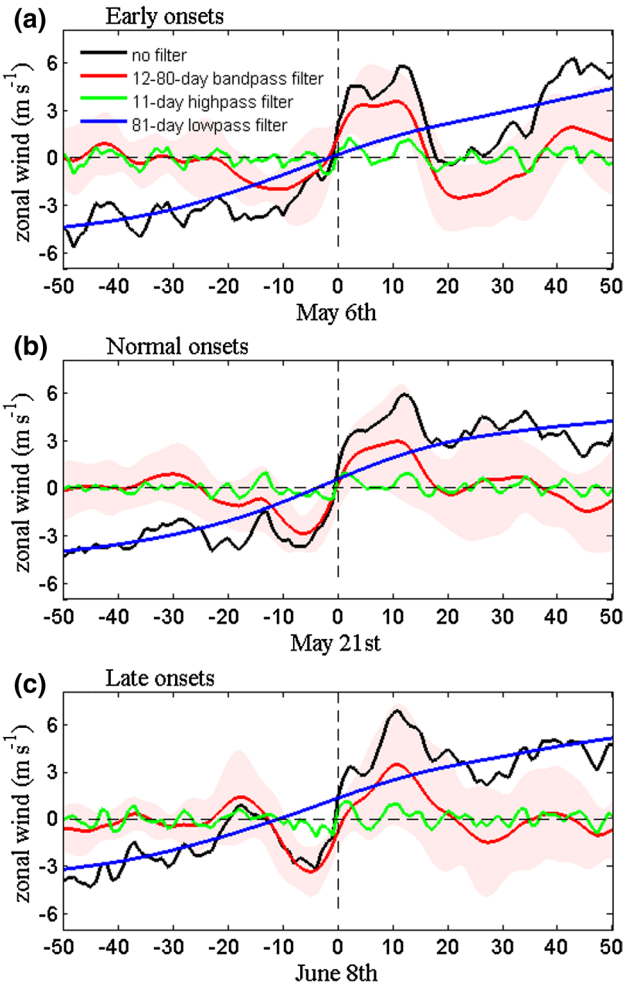

Fig. 2 Different components of three types of SCSSM onsets. Evolution of composite total (black), 12–80-day bandpass-filtered (red), 11-day highpass-filtered (green) and 81-day lowpass-filtered (blue) U850 averaged over the SCS (110°E–120°E; 5–15°N) from day −50 to day 50 for **a** 9 early onsets, **b** 15 normal onsets and **c** 10 late onsets. Day 0 denotes the onset day. The shadings indicate the standard deviations of the 12–80-day bandpass-filtered U850 in each onset. The mean early onset date is May 6th, the mean normal onset date is May 21st and the mean late onset date is June 8th

4 Local ISO-SCSSM onset relationship

To study the roles of different time-scale variabilities on the SCSSM onset, the SCSSM index, defined by the SCS-averaged 850-hPa zonal wind, is decomposed into three time scales. The intraseasonal wind anomaly is obtained by performing 12–80-day bandpass filtering, the seasonal wind anomaly, by 81-day lowpass filtering and the synoptic anomaly, by the original data minus the 11-day lowpass-filtered anomaly. The sum of these synoptic, intraseasonal and seasonal signals nearly equals (above 94%) to the total wind.

Figure 2 shows the composite SCSSM index on different time scales with respective to these three types of SCSSM onsets. For each onset, the onset date is set as "day 0", and a window with 50 days before and 50 days after the onset is used for the composite. For all three types of onsets, the total zonal wind changes from negative to positive on the onset day, i.e., day 0, which denotes the outbreak of the westerly following the definition of the SCSSM onset. Before the early onset (Fig. 2a), a negative intraseasonal wind anomaly lasting 28 days is observed. At the onset day of the early onset (Fig. 2a), both seasonal and synoptic westerly wind anomalies over the SCS, are very weak, which are only 0.16 and 0.52 m s^{-1}, respectively, occupying only 7.3 and 23.8% of the total wind anomalies. The total westerly wind anomaly of 2.18 m s^{-1} is mainly induced by the intraseasonal

westerly wind anomaly of 1.35 m s^{-1}. After the onset, the continuous westerly wind anomalies are also sustained by the intraseasonal wind anomalies. For the 20-day-averaged wind anomalies after the onset, the ratio of the intraseasonal wind anomaly to the total westerly wind anomaly is 58.6%, while the ratio is only 33.5% for the seasonal wind anomaly, and 6.6% for the synoptic-scale anomaly.

For the normal onset day (Fig. 2b), the total westerly wind anomaly of 1.37 m s^{-1} comes mainly from the seasonal and synoptic westerly wind anomalies. The seasonal westerly wind anomaly, synoptic wind anomaly and intraseasonal wind anomaly are 0.53, 0.58 and 0.23 m s^{-1}, respectively; and their ratios to the total westerly wind anomaly are 38.7, 42.3 and 16.8%, respectively. We conclude that the normal onset is triggered by synoptic signal in conjunction with seasonal evolution when the negative ISO loses its control over the SCS. After the onset, the continuous westerly wind anomalies are mainly contributed by the seasonal and intraseasonal oscillations, the ratio of the 20-day-averaged seasonal, intraseasonal, and synoptic wind anomalies to the total westerly wind anomaly are 45.4, 45.4 and 6.1%, respectively. Before the onset, a long-term negative phase of the intraseasonal SCSSM index also appears for about 25 days.

For the onset date of the late onset cases, the total westerly wind anomaly of 1.44 m s^{-1} mainly comes from the seasonal wind anomaly of 1.33 m s^{-1}, and secondly from the synoptic anomaly of 0.67 m s^{-1}. The intraseasonal wind anomaly, however, is negative. This means that these late onsets are also triggered by the combination of seasonal and synoptic anomalies when the negative ISO becomes weak. After the onset, the intraseasonal anomaly helps to sustain the SCSSM. The ratio of the 20-day-averaged seasonal, intraseasonal, and synoptic wind anomalies to the total westerly wind anomaly are 54.0, 39.6 and 5.4%, respectively. Before the onset, there exists a strong negative phase of ISO with a period of 12 days.

In summary, there is a long-term negative phase of the ISO, denoted by the intraseasonal easterly wind anomalies over the SCS, before each of these three types of onsets. This negative ISO is shortest for the late onsets among these three types of onsets. All these three types of onsets are accompanied by the dry-to-wet phase transition of the SCS ISO, while the early onsets are mainly triggered by the intraseasonal westerly anomaly, the normal and late onsets are triggered by the seasonal and synoptic westerly anomalies, consistent with the finding (Shao et al. 2014). The intraseasonal easterly wind anomaly on the onset day is not favorable for a late onset. After surveying all these three types of onsets, the intraseasonal westerly wind anomaly is favorable for sustaining the SCSSM, whose role is the strongest for the early onsets and the weakest for the late onsets.

This conclusion is method-dependent. By using a 3-day running mean to obtain the subseasonal variability (Wu 2010), the quasi-biweekly oscillation has been found to be important to trigger the SCSSM onset. In this work, when using a 9–25-day butterworth bandpass filter, the obtained quasi-biweekly oscillation occupies 12.3, 33.0 and 25.2% of the total wind for the early, normal and late onsets, respectively, which means that the quasi-biweekly oscillation is also important for triggering the SCSSM onset, consistent with the work of Wu (2010). When we use a normal 12–25-day bandpass filter to obtain the quasi-biweekly oscillation, the westerly anomaly is relatively small, i.e., occupying 4.8, 13.7 and 10.1% of the total westerly anomaly for the early, normal and late onsets, respectively, while the synoptic signal is strong and dominates the normal and late onsets.

5 Characteristics of ISO related to different SCSSM onsets

To understand these effects discussed in Sect. 4, the evolution of the ISO during SCSSM onset is discussed next. The OLR, a good index for ISO convection, will be used to show the ISO evolution, as well as the 850-hPa wind that is well coupled to the ISO convection.

5.1 Early onset years

Figure 3 shows the composite evolution pattern of 12–80-day-filtered 850-hPa wind and OLR anomalies from 20 days before to 16 days after these nine early SCSSM onsets. Day 0 denotes the onset day of the SCSSM when the easterly turns to the westerly wind anomalies over the SCS.

Before the early onset, the active ISO convection anomaly is initiated in the central equatorial Indian Ocean at day − 20, and propagates eastward accompanied by an increasing westerly anomaly from day − 20 to day − 12. From day − 8 to day − 4, the ISO continues to propagate eastward and reaches the western Pacific after passing over the Maritime Continent. The Rossby component of the ISO is left behind in the Indian Ocean, and its northern part propagates northward into the Bay of Bengal. Among the nine early SCSSM onset years, six Bay of Bengal monsoon onsets led the SCSSM onset by less than 10 days (Fig. 1), and they are found to be related to this wet ISO. The Bay of Bengal monsoon onsets triggered by the first northward propagation branch of the ISO were well discussed by Li et al. (2012, 2015). At day 0, the Rossby component of the western Pacific ISO propagating northwestward increases the convection over the SCS and triggers the onset of the SCSSM. The wet phase of the ISO over the SCS is enhanced and continues from day 0 to day 12. At day 16, the SCS ISO changes into its dry phase, while the seasonal westerly anomaly is strong enough to maintain the SCSSM (Fig. 2a). Ten days before the onset, the quasi-biweekly

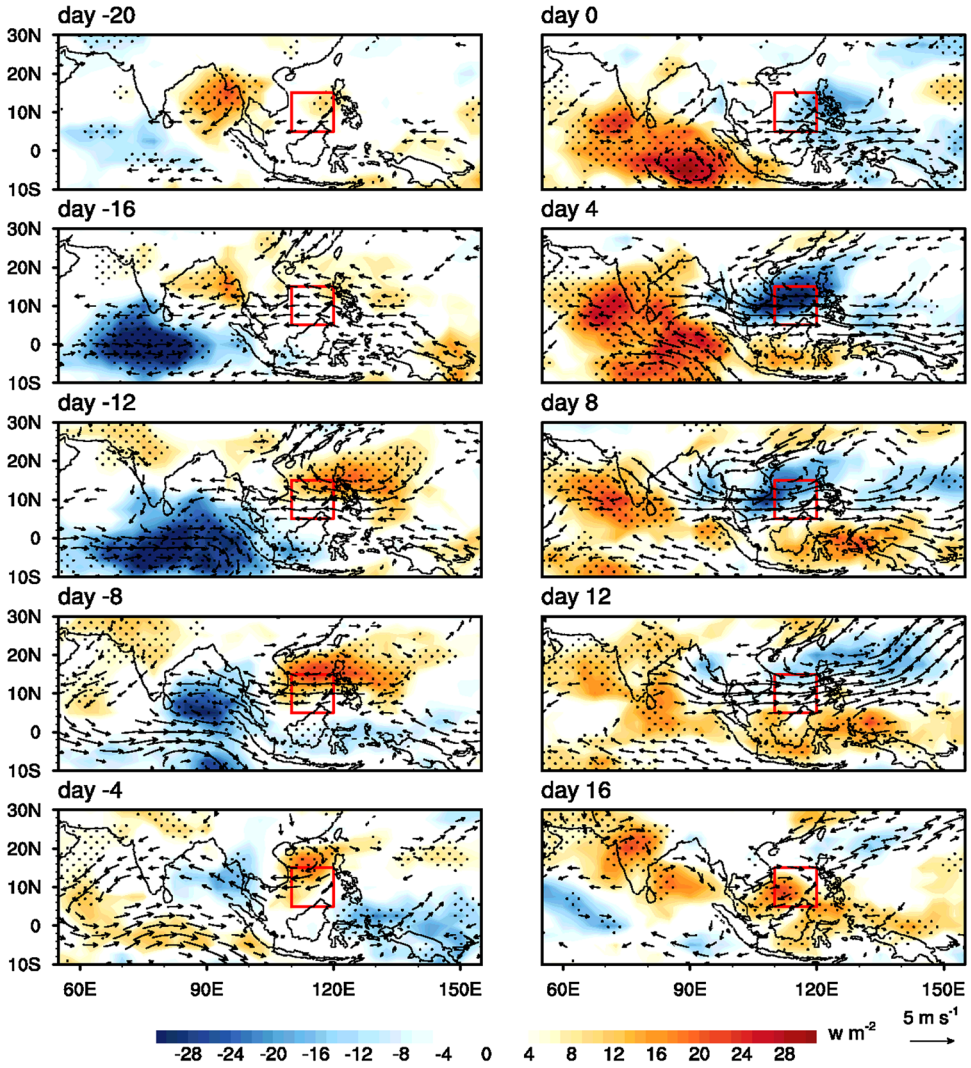

Fig. 3 ISO evolution associated with early SCSSM onset. Evolution of composite 12–80-day bandpass-filtered 850-hPa wind (vector) and OLR (shaded) from day −20 to day 16 for the 9 selected early onsets. Day 0 denotes the onset day. Stippling indicates OLR anomalies over the 95% significant level, based on the *t* test. Wind anomalies above 1 m s^{-1} are only plotted

oscillation was also found to originate from the western equatorial Pacific (Wu 2010). By analyzing the 12–25 and 30–60 day signals separately, we found the weak quasi-biweekly oscillation can originate from the western equatorial Pacific, while the strong 30–60 day ISO does come from the Indian Ocean (not shown).

Before the onset (of day 0), the dry phase of ISO appears over the SCS since day −16, which is related to the easterly wind anomalies of the wet phase of the ISO over the tropical Indian Ocean. This dry ISO phase prior to the onset may cause SST warming and precondition the onset of the SCSSM, consistent with the result of Wu (2002). From day −4, a negative convection anomaly is also initiated from the western tropical Indian Ocean, which tends to propagate eastward. After the onset, this dry ISO phase over the Indian Ocean also enhances the convection over the SCS and sustains the SCSSM. The dry ISO over the tropical Indian Ocean and the wet ISO over the SCS constitute a positive feedback, through the local Walker circulation, similar to the positive feedback between the ISO over the Indian summer monsoon and tropical Indian Ocean (Liu and Wang 2012).

In a word, strong ISO initiated from the equatorial Indian Ocean can pass over the Maritime Continent and reach the western Pacific, whose Rossby component then triggers the SCSSM onset in these early onset years. The local Walker circulation between the tropical Indian Ocean and SCS can precondition the outbreak of the SCSSM before the onset and sustain the SCSSM after the onset.

5.2 Normal onset years

The composite evolution pattern in normal onset years is similar to that in early onset years, but there are some notable differences between the two (Fig. 4). Before the normal onset, the active ISO convection initiated in the western equatorial Indian Ocean at day −20 mainly propagates eastward from day −20 to day −8. From day −8, however, this wet ISO mainly propagates northward into the southern Bay

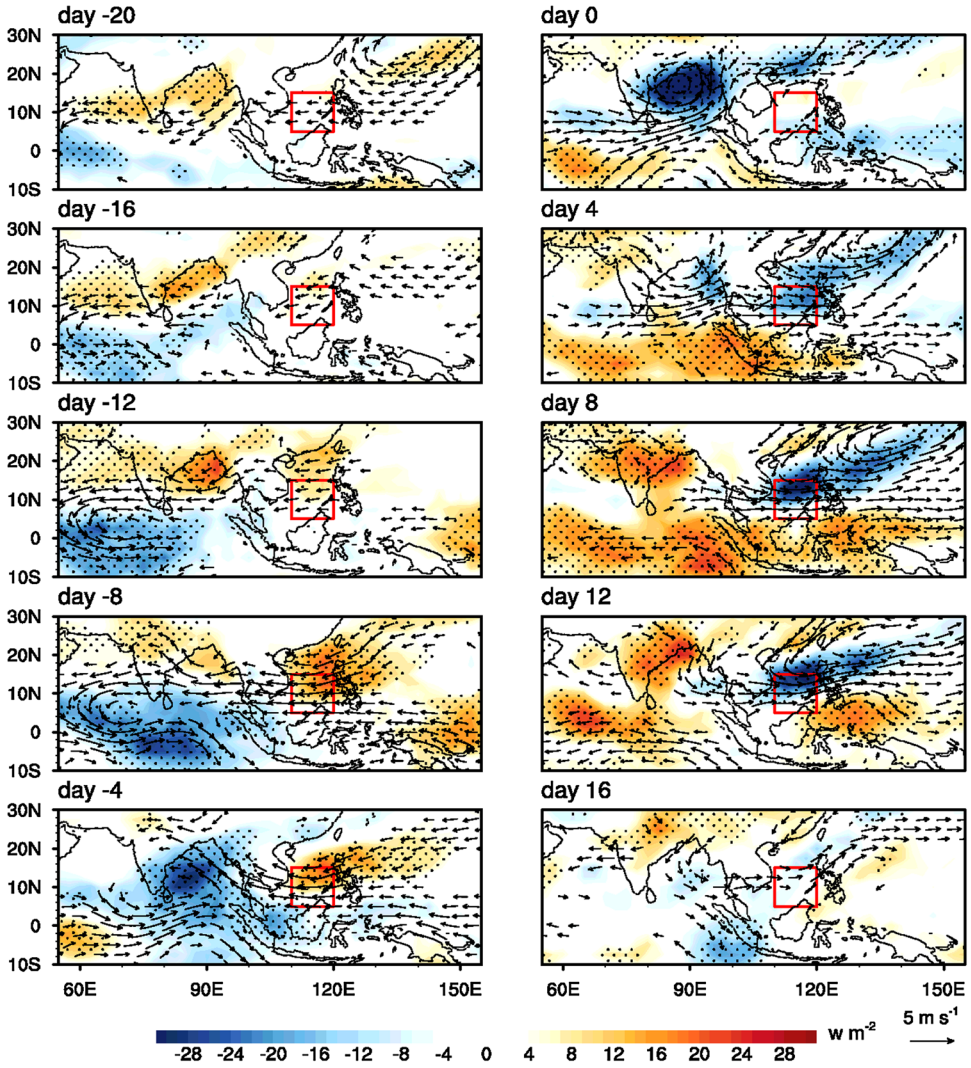

Fig. 4 ISO evolution associated with normal SCSSM onset. Same as in Fig. 3, except for normal onsets

of Bengal. At day 0, the wet ISO reaches its maximum in the northern Bay of Bengal, i.e., north of 10°N. At the same time, positive convective activities with strong westerly anomalies are excited over South China, since the convective latent heating release over the Bay of Bengal can excite an asymmetric Rossby wave, inducing the intrusion of the mid-latitude trough (Liu et al. 2002). For this convection to the north of 10°N, the Kelvin wave response of the Gill pattern disappears and the associated easterly wind anomalies also disappear from the Bay of Bengal to the SCS. This disappearance of Kelvin wave response has been confirmed by an intermediate model simulation (Liu and Wang 2013). The equatorial part of this wet ISO also passes over the Maritime Continent and reaches the western Pacific at day 0. A strong 12–25-day ISO also originates from the western equatorial Pacific at day 0 (not shown), consistent with the result of Wu (2010). The SCSSM onset is mainly triggered by the seasonal and synoptic-scale variabilities (Fig. 2b). After the onset, the wet ISO over the Bay of Bengal decays quickly, and the westerly anomaly over the northern part of the SCS shows a southward shift and enhances the rainfall over the SCS at day 4, consistent with previous findings (Chang 1995; Chan et al. 2000; He et al. 2006). This southwest-northeast tilted rain band lasts to day 16 over the SCS.

Before the onset, the dry phase of SCS ISO preconditioning the onset appears from day −20 to day −4, associated with the northeastward propagation of wet ISO from the Indian Ocean to the southern Bay of Bengal. The dry ISO evolution from the Indian Ocean to the southern Bay of Bengal also supports the SCSSM through its westerly wind anomalies from day 0 to day 12.

Different from the early onset year when the SCSSM onset is related to the eastward propagation of the ISO along the equator, the normal onset is closely related to the northeastward propagation of the ISO from the Indian Ocean to the Bay of Bengal. Before the normal onset around May 21st, the Bay of Bengal monsoon has been established for about 20 days, and the vertical easterly wind shear may favor

the northward propagation of the ISO (Jiang et al. 2004). In Fig. 4, the lower-tropospheric easterly wind anomaly over the Bay of Bengal before day −4 demonstrates a negative ISO phase, while the seasonal mean in the lower troposphere is the westerly. The normal onset is triggered by the seasonal and synoptic-scale westerly anomalies. Then the normal onset is mainly supported by the southward moving convection associated with the front from South China when the wet ISO moves to the northern Bay of Bengal and becomes weakened.

5.3 Late onset years

Figure 5 shows the composite evolution pattern for 10 late onset years, and the pattern of ISO propagation is much different from that of early and normal onset years. From day −20 to day −4, the active convection anomaly of ISO initiated from the western equatorial Indian Ocean mainly propagates northward to the Arabian Sea and triggering nine Indian summer monsoon onsets among the ten late SCSSM onset years, as mentioned in some studies (Wang et al. 2009a, b; Zhou and Murtugudde 2014). Strong easterly wind anomalies are excited from the SCS to the Arabian Sea, associated with this strong southern Indian summer monsoon to the south of 10°N. At day 0, the wet phase of ISO moves to the northern Indian monsoon region, i.e., to the north of 10°N, and is weakened. This is followed by a new dry ISO phase, which moves northeastward. Thus the easterly wind anomalies from the SCS to the Arabian Sea become weakened and the SCSSM onset is triggered by the synoptic-scale variability (Fig. 2c). After the onset, strong ISO westerly wind anomalies appear across the broad region from the Arabian Sea to the SCS from day 4 to day 16. Compared to the strong westerly wind anomaly, the rainfall is relatively weak after the late onset (Fig. 5). The weak coupling between the circulation and convection over the SCS inspires our rethinking of the onset definition.

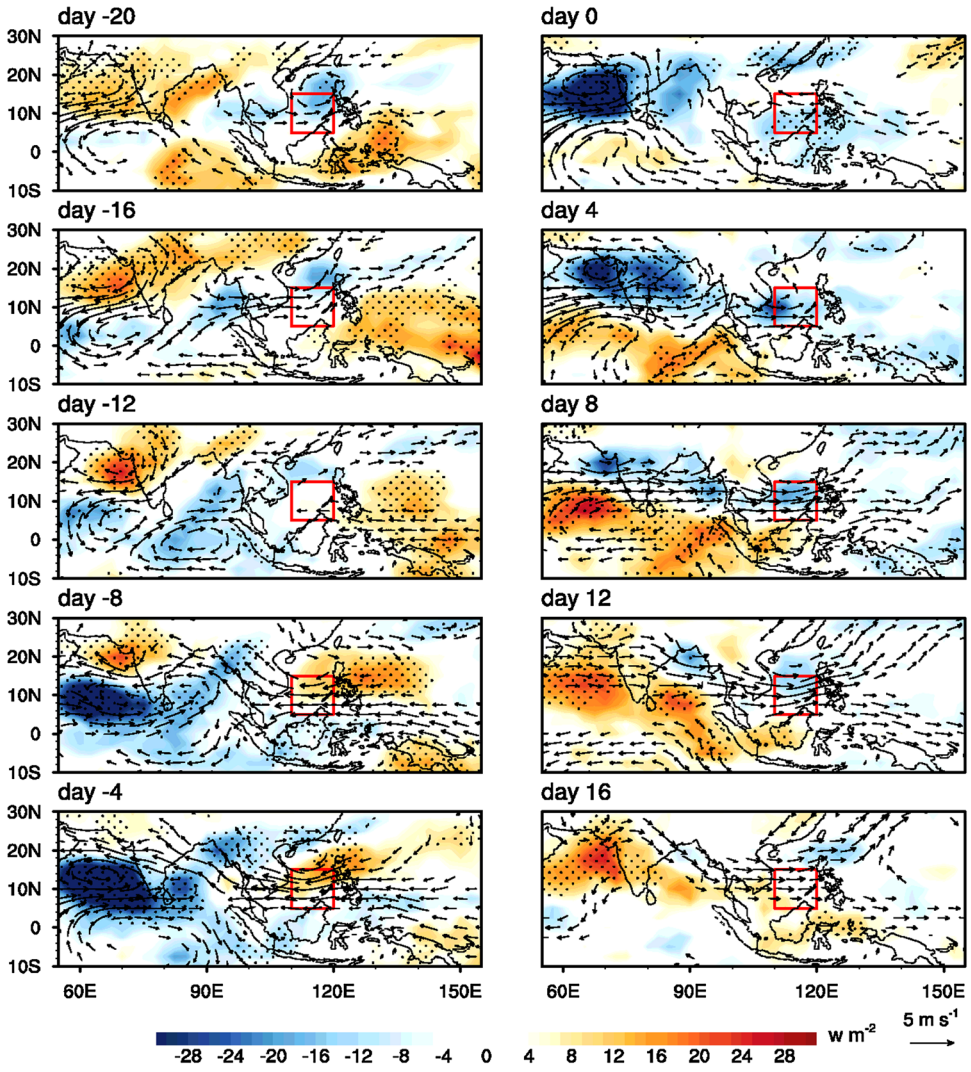

Fig. 5 ISO evolution associated with late SCSSM onset. Same as in Fig. 3, except for late onsets

Before the late onset, the dry phase of the SCS ISO preconditioning the onset only appears from day −8 to day −4, which is much shorter than that in the early and normal onset years. This dry phase is mainly caused by the wet ISO over the southern Indian monsoon region. After the onset, the westerly wind anomalies across the Arabian Sea to the SCS associated with the dry ISO from the western Indian Ocean to the southern Indian monsoon region will support the SCSSM.

For these late onsets around June 8th, seasonal westerly anomalies are strong, while the strong wet phase of the ISO of the southern Indian summer monsoon will delay the SCSSM onset through the easterly wind anomaly across the whole Arabian Sea, the Bay of Bengal and the SCS. The SCSSM onset can only be excited by synoptic-scale variability when the wet ISO moves to the northern Indian summer monsoon and becomes weak.

5.4 Similar and different features

For all three types of onsets, the SCSSM westerly wind bursts and SCSSM onsets are closely accompanied by the transition of ISO from dry phase to wet phase. For all the onsets, there is a warming-cooling evolution in SSTa (Fig. 6). Before each of these three types of onsets, the SCS is controlled by the dry phase of the ISO, which lasts more than 20 days for both early onsets and normal onsets, and 10 days for the late onsets. Associated with the dry phase of the ISO, the SCS is warmed and its SST reaches the peak before the onset. After the onset, the SCS is dominated by the wet phase of the ISO associated with decreasing SST. An anti-correlation exists for the ISO between the SCS and Indian Ocean, which should constitute a positive feedback (Liu and Wang 2012). The local low-level easterly Walker circulation constitutes a positive feedback to precondition the SCS leading to onset, while the low-level westerly Walker circulation constitutes a positive feedback to support the SCSSM. Previous studies (Liang et al. 1999; Zhou and Chan 2007) showed that in late (early) SCSSM onset years, the intensity of the SCSSM tends to be weaker (stronger). This conclusion can also be drawn based on the different strengths of OLR from Fig. 6.

The ISO evolutions related to these three types of onsets are different. In the early onset years, the ISO over the SCS is mainly related to the eastward moving ISO along the equatorial Indian Ocean (Fig. 3), while in the normal onset years, it is related to the northeastward ISO propagation from the equatorial Indian Ocean to the Bay of Bengal (Fig. 4), and in the late onset years, to the northward ISO propagation from the equatorial Indian Ocean to the Indian summer monsoon region (Fig. 5).

The trigger mechanisms for these three types of onsets are also different. In the early onset years, the ISO initiated

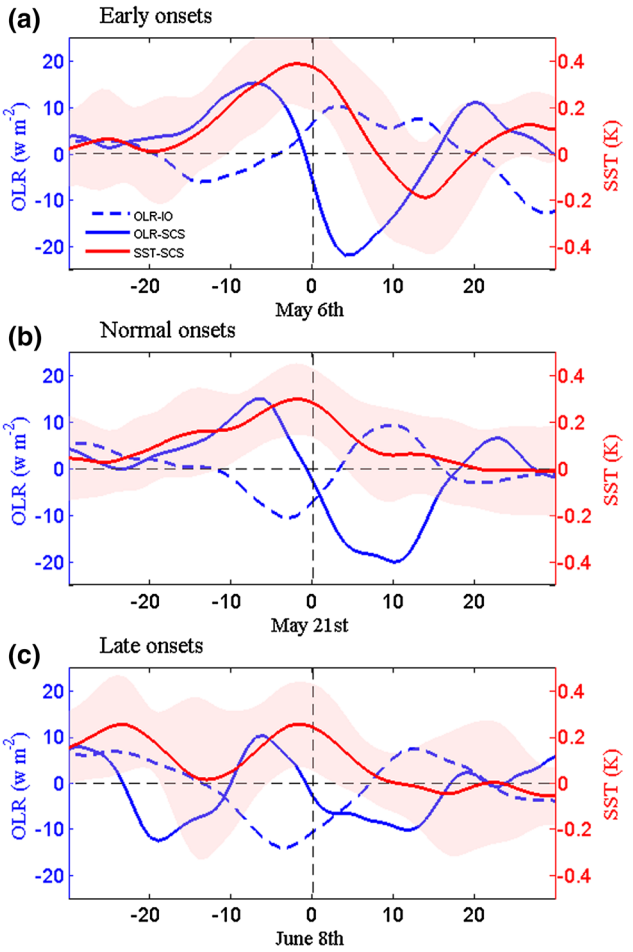

Fig. 6 Air-sea interaction for different onsets. Evolution of composite 12–80-day bandpass-filtered OLR averaged over the SCS (solid blue line) and over the Indian Ocean (60°E–100°E, 0–25°N; dashed blue line), as well as SST over the SCS (solid red line) from day −30 to day 30 for **a** 9 early onsets, **b** 15 normal onsets and **c** 10 late onsets. Day 0 denotes the onset day. The shadings indicate the standard deviations of the 12–80-day bandpass-filtered SST over the SCS in each onset

from the equatorial Indian Ocean propagates eastward to the western Pacific; then its wet Rossby gyre moves northwestward to trigger the SCSSM onset. In the normal onset years, the onsets are triggered by the seasonal and synoptic-scale variabilities when the wet ISO moves to the northern Bay of Bengal monsoon region and the Kelvin wave response of the Gill pattern disappears. Meanwhile, a southwest-northeast tilted front over South China, excited by the convection over the Bay of Bengal, will move southward to support the SCSSM onset. While in the late onset years, the SCSSM onset is excited by the synoptic-scale variability under the seasonal westerly anomalies when the wet ISO moves to the northern Indian monsoon region and the easterly anomaly of the Kelvin wave response disappears.

6 Mechanisms for different ISO evolutions

To understand different ISO evolutions associated with these three types of SCSSM onsets, we address the following questions: (1) In early May, why can the ISO originating from the Indian Ocean trigger the SCSSM onset only in the early onset years, not in the normal or late onset years? (2) In late May, why does the ISO not trigger the SCSSM onset in the late onset years? (3) In early June, why does the ISO prefer propagating northward to the Arabian Sea to trigger the Indian summer monsoon rather than propagating eastward or northeastward in the late onset years? Since the evolution of the ISO has been found to be controlled by the mean state (Wang and Xie 1996; Jiang et al. 2004; Li et al. 2012; Liu et al. 2015a, b, 2016b), the ISO evolutions and associated mean states will be investigated next.

6.1 Around May 6th

To understand why the ISO originating from the Indian Ocean can trigger an early SCSSM onset, but not normal or late onset during early May, we use Fig. 7 to show different ISO evolutions around May 6th for the early onset years and the years for the other onset types. Day 0 of a selected ISO event is defined when the equatorial Indian Ocean (65°E–75°E, 5°S–5°N) averaged OLR anomaly reaches its minimum during April 16th to May 6th and this minimum should be less than − 15 w m^{-2}. In the beginning from day 0 to day 5, the ISO mainly propagates eastward along the equator for all years, associated with the easterly wind anomalies excited over the SCS. This easterly anomaly is much stronger in the early onset years than in the other years. By day 10, the equatorial part of the ISO passes over the Maritime Continent and reaches the western Pacific, while the Rossby gyre moves northward to the Bay of Bengal. At day 15, the strong wet phase of the ISO appear over

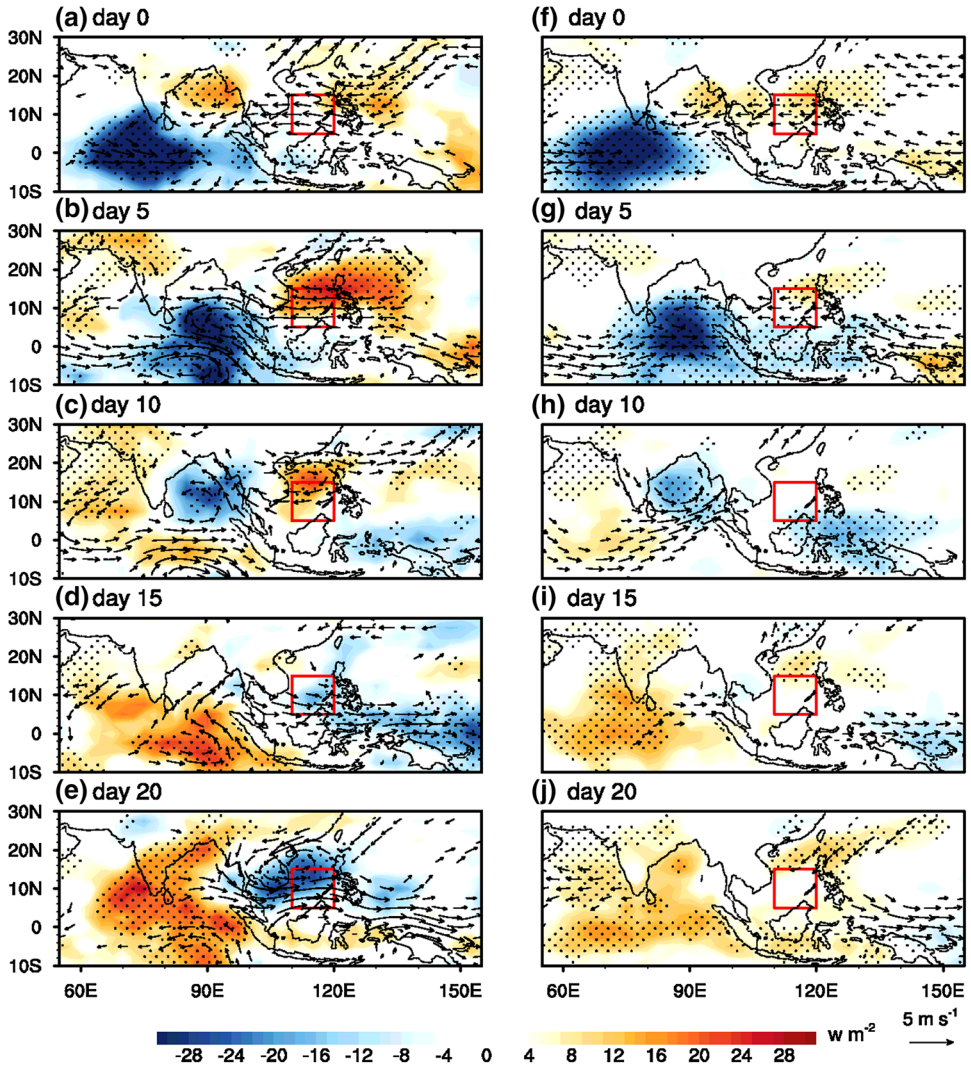

Fig. 7 ISO evolution before May 6th. Evolution of composite 12–80-day bandpass-filtered 850-hPa wind (vector) and OLR (shaded) from day 0 to day 20 for the ISO initiated from the western Indian Ocean for nine early onset years (left panels) and the other 25 years (right panels). Day 0 denotes the day when the OLR anomaly averaged over the western Indian Ocean (65°E–75°E, 5°S–5°N) reaches a minimum during the April 16th to May 6th period. Stippling indicates OLR anomalies over the 95% significant level, based on the t-test. Wind anomalies above 1 m s^{-1} are only plotted

the SCS and western Pacific in the early onset years, and the dry ISO in the Indian Ocean tends to support the rainfall over the SCS. In the other years, however, the signal in the SCS and western Pacific decays quickly. Although the dry ISO in the Indian Ocean tries to support the westerly wind anomalies over the SCS, no rainfall associated with the ISO occurs over the SCS.

To understand these different evolutions of the ISO, Fig. 8 shows the associated mean states, including convective instability, SSTa, lower-tropospheric moisture and convergence during April 16th -May 6th in these early and other onset years. In the early onset years, there is a positive convective instability anomaly, associated with warm SSTa over the western North Pacific before May 6th (Fig. 8a), which is favorable for the growth of the ISO. Positive moisture and convergence anomalies over the SCS also help ISO development (Fig. 8c). This positive feedback of warm SSTa and large moisture anomaly on the ISO over the western North Pacific was revealed by Liu et al. (2016b). In the normal and late onset years, the mean state exhibits strong negative convective instability anomaly and cool SSTa (Fig. 8b), as well as, a negative moisture anomaly (Fig. 8d) before May 6th over the western North Pacific, and the associated seasonal-mean easterly wind anomaly is also strong during this period (Fig. 2b, c). These negative mean states will suppress the development of the ISO over the western North Pacific. The warm western North Pacific in the early onset years can be attributed to the interannual (Wu and Wang 2000; Liang et al. 2013) or decadal (Yuan and Chen 2012; Xiang and Wang 2013) La Niña-like SST pattern. Thus, the interannual-to-decadal variability in the western North Pacific will modulate the ISO evolution, and then control the SCSSM onset.

6.2 Around May 21st

The second issue should be addressed is why the ISO can affect the SCSSM onset around May 21st in the normal onset years, but not in the late onset years. Figure 9 shows the ISO evolutions around May 21st for the normal and late onset years. In the normal onset years, the ISO initiated from the western Indian Ocean propagates eastward from day 0 to day 5, and it is mainly dominated by the Rossby gyre over the southern Bay of Bengal at day 10. From day 5 to day 15, one signal propagates from the western equatorial Pacific to the SCS, and a weak front moves southward over the western North Pacific. Compared to the strong front over South China associated with the strong ISO over the Bay of Bengal in Fig. 4, the front here is relatively weak, as well as the Bay of Bengal ISO, which means that only part of the ISO originating from the western Indian Ocean can propagate northeastward to affect the Bay of Bengal.

In the late onset years, the ISO over the Indian Ocean and western Pacific is relatively weak, and no large-scale

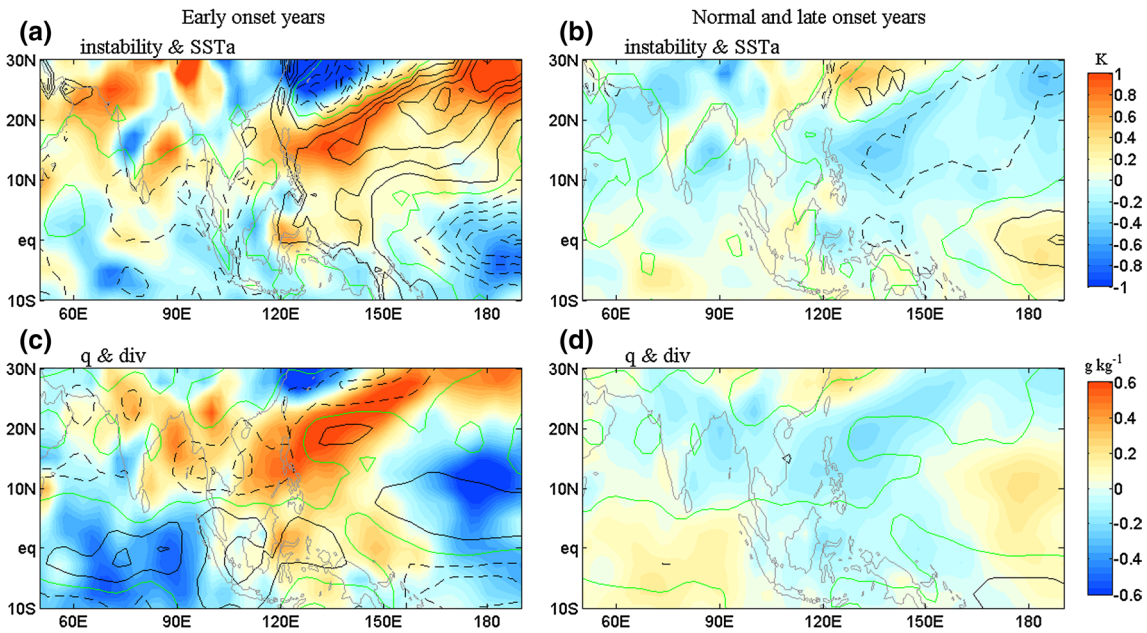

Fig. 8 Mean states before May 6th. Shown are the composite 81-day low-pass-filtered convective instability (θe, shading; K) and SSTa (contour; K) averaged for the period of April 16th to May 6th for **a** nine early-onset years and **b** the other 25 years. The convective instability is defined by the difference of equivalent potential temperature between lower (1000 – 700 hPa) and mid (600 – 300 hPa) troposphere. **c, d** are the same as **a, b**, except for 850-hPa moisture (shading; g kg^{-1}) and divergence (contour; s^{-1}*10^{-4}). The green contour denotes zero, and the contour intervals are 0.1K for SSTa and s^{-1}* 10^{-5} for divergence

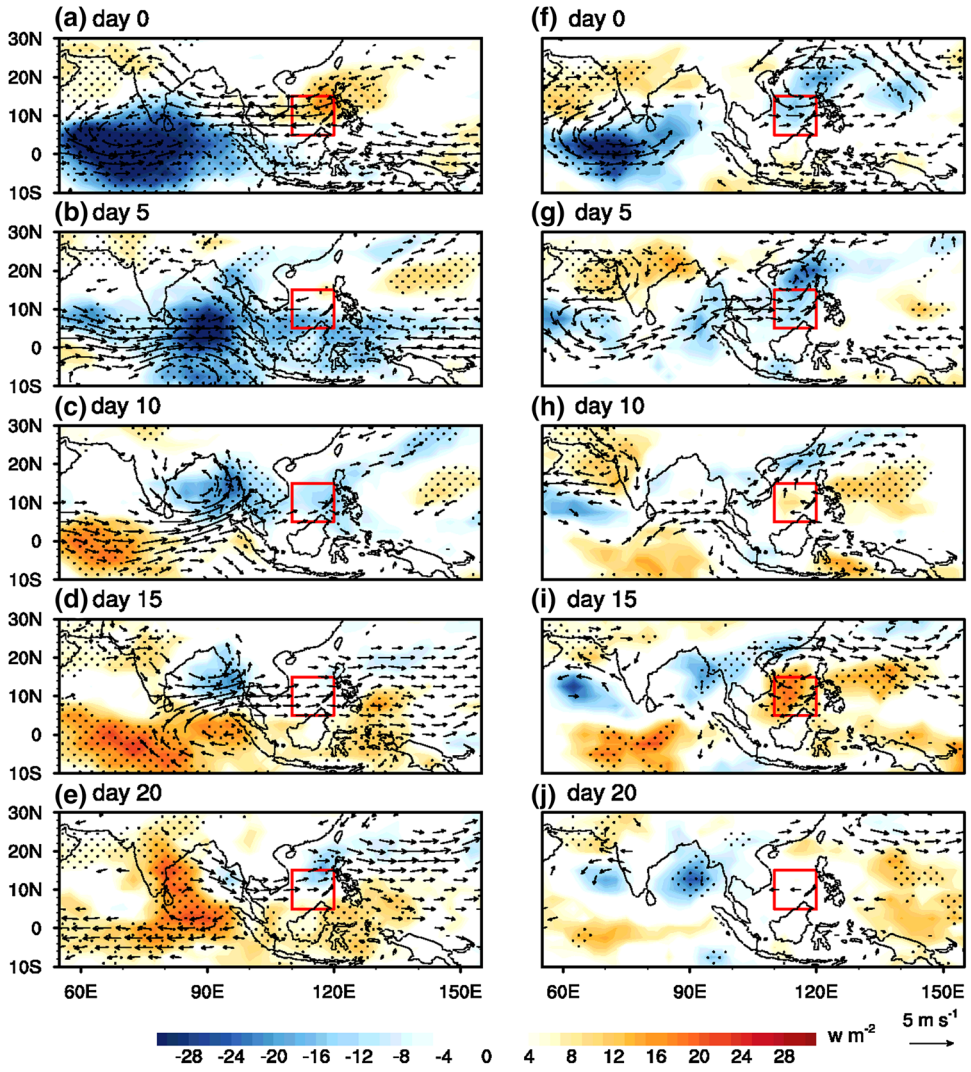

Fig. 9 ISO evolution before May 21th. Evolution of composite 12–80-day bandpass-filtered 850-hPa wind (vector) and OLR (shaded) from day 0 to day 20 for the ISO initiated from the western Indian Ocean for 15 normal onset years (left panels) and 10 late onset years (right panels). Day 0 denotes the day when the OLR anomaly averaged over the western Indian Ocean (65°E–75°E, 5°S–5°N) reaches a minimum during the May 1st to May 21th period. Stippling indicates OLR anomalies over the 95% significant level, based on the *t* test. Wind anomalies above 1 m s^{-1} are only plotted

circulation-convection coupled system can be found. The convection over both Indian Ocean and SCS is coupled with the westward propagating Rossby gyre. After day 10, the SCS is dominated by the intraseasonal easterly wind anomaly. Since the seasonal easterly wind anomaly is still strong during May 1st to 21st in the late onset years (Fig. 2c), the SCSSM onset cannot be triggered.

Different from the normal onset years (Fig. 10a, c), the mean states for the period from May 1st to 21st experience strong negative convective instability anomaly, cold SSTa, negative moisture anomaly, and strong divergence anomaly over the northern Indian Ocean and western North Pacific in late onset years (Fig. 10b, d). Thus, the ISO is much suppressed and minimally impacts the SCSSM onset during late onset years.

6.3 Around June 8th

The last question to be addressed is why the ISO over the Indian Ocean propagates northward to the Arabian Sea to trigger the Indian summer monsoon and delay the SCSSM onset rather than propagates eastward to trigger the SCSSM onset directly around June 8th in the late onset years. Figure 11 shows the background convective instability and vertical wind shear anomaly during the period of May 19th to June 8th in the late onset years. A strong northward gradient of the background convective instability with maximum convective instability over the land is found during this period. Previous studies have shown that the poleward gradient of convective instability could produce poleward propagation of convective anomalies (Webster and Chou 1980;

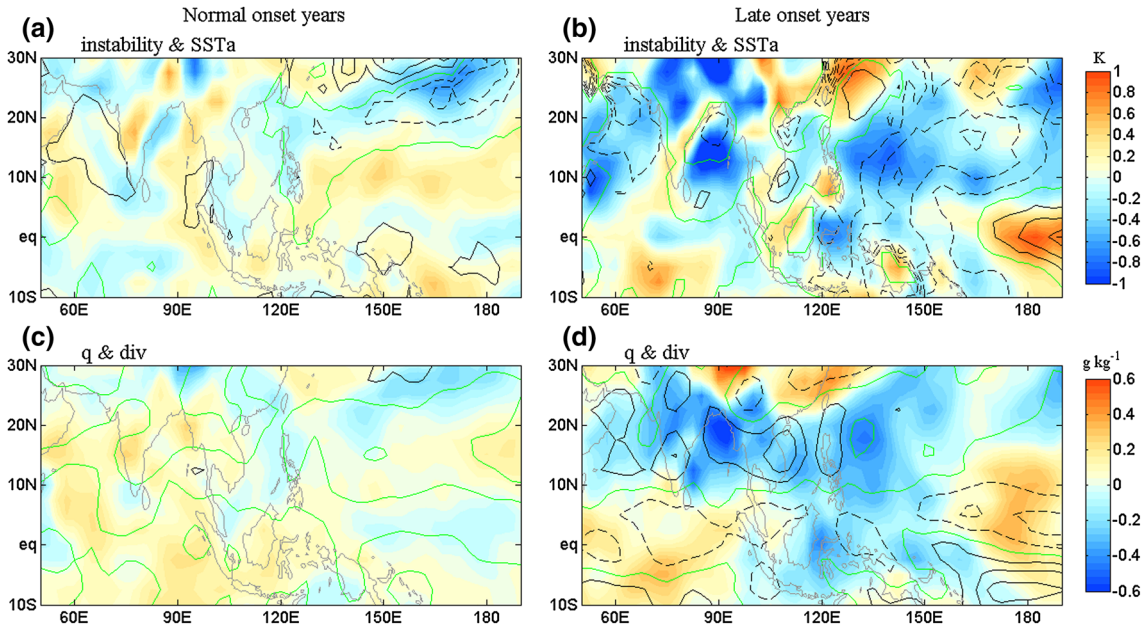

Fig. 10 Mean states before May 21st. Shown are the composite 81-day low-pass-filtered convective instability (θe, shading; K) and SSTa (contour; K) averaged for the period of May 1st to May 21st for **a** 15 normal-onset years and **b** 10 late-onset years. **c, d** are the same as **a, b**, except for 850-hPa moisture (shading; g kg^{-1}) and divergence (contour; $s^{-1}{\cdot}10^{-4}$). The green contour denotes zero, and the contour intervals are 0.1 K for SSTa and $s^{-1}{\cdot}10^{-5}$ for divergence

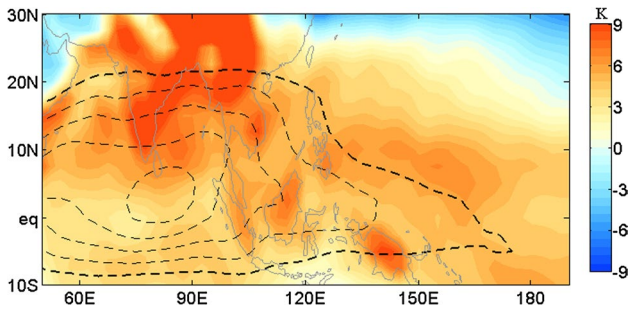

Fig. 11 Mean state before June 8th. Shown is the composite 81-day lowpass-filtered convective instability (θe, shaded, K) and vertical wind shear (U200–U850, contours, m s^{-1}) averaged for the period of May 19th to June 8th for 10 late onset years. Only easterly shear is contoured by dashed line, and the thick dashed line denotes zero. Counter interval is 5 m s^{-1}

Srinivasan et al. 1993). Since the Bay of Bengal monsoon has been established in this period, a strong climatological easterly vertical wind shear also occurs over the Indian Ocean. This easterly vertical shear prefers the northward propagation of the ISO through exciting the barotropic vorticity anomaly to the north of the convective center (Kemball-cook and Wang 2001; Jiang et al. 2004; DeMott et al. 2013; Liu et al. 2015a, b). By these mechanisms, the ISO initiated from the western Indian Ocean propagates northward to trigger the Indian summer monsoon. Around June 8th during early- and normal-onset years, similar northward gradient of the background convective instability and easterly vertical wind shear as those in Fig. 11 exist (not shown). Thus, the ISO also experiences the northeastward propagation over the Indian Ocean. During early-May, the northward propagation of the ISO also triggers the Bay of Bengal summer monsoon, mainly through the poleward gradient of convective instability in the eastern Indian Ocean, since the easterly vertical wind shear is not yet established at that time (Li et al. 2012).

7 Summary and discussion

To improve the extended-range forecast of SCSSM onset, we document different effects of the ISO on early, normal and late SCSSM onsets. For all three types of onsets, a warming-cooling evolution in SSTa is found (Figs. 2, 6). Before each onset, the SCS is controlled by the dry phase of the ISO (Shao et al. 2014), and the SCS is warmed to precondition the onset. After each onset, the SCS is cooled by the wet phase of the ISO. This local warming-cooling evolution, discovered by Wu (2010), confirms the extended-range forecast source for the SCSSM onset prediction. The transition process, however, is found to be related to different ISO evolutions over the Indian Ocean for the three types of onsets. For the early onset, the dry/wet phase of SCS ISO is supported by the easterly/westerly wind anomaly related to the wet/dry phase of the ISO propagating eastward along the equatorial Indian Ocean (Fig. 3), while it is related to the

ISO propagating northeastward from the equatorial Indian Ocean to the Bay of Bengal monsoon region for the normal onset (Fig. 4), and to the northward propagating ISO from the tropical Indian Ocean to the Indian monsoon region for the late onset (Fig. 5).

The early onset is found to be triggered by the Rossby gyre of the wet phase of ISO over the western Pacific coming from the Indian Ocean. The normal onset is triggered by the synoptic-scale activity when the wet ISO moves to the northern Bay of Bengal monsoon region, since the convection to the north of 10°N cannot excite the easterly anomaly of Kelvin wave responses to suppress the SCS convection. At the same time, the southward moving front from South China excited by the Bay of Bengal convection will support the SCSSM onset. The late onset, however, is delayed by the wet phase of the southern Indian summer monsoon ISO, and is triggered by the synoptic-scale variability when the dry phase of SCS ISO caused by the strong southern Indian summer monsoon is weakened. Here, these different onset processes, i.e., the ISO triggering process (Mao and Chan 2005; Zhou and Chan 2005; Straub et al. 2006), the front triggering process (Chen and Chen 1995; Chan et al. 2000; Ding and Liu 2001; Tong et al. 2008), and the synoptic variability triggering process (Mao and Wu 2008), are selected by mean state-modulated ISO evolutions.

These different ISO evolutions and SCSSM onsets are modulated by the mean-state convective instability. A warm and moist western North Pacific will favor the eastward propagation of the ISO and advance the SCSSM onsets, while a cold and dry one tends to suppress the ISO and delay the SCSSM onset. The ENSO and Pacific Decadal Oscillation (PDO) related western North Pacific SST will provide a predictability source to identify the type of ISO evolution before the onset, and the ISO signal initiated over the western Indian Ocean will provide a predictability source for the extended-range forecast of the SCSSM onset. This prediction system is being built and tested.

The advance of the Asian summer monsoon rain band has been well studied (Lau and Yang 1997; Webster et al. 1998; Wang and LinHo 2002), and the climatological onset of the Asian summer monsoon first occurs over the Bay of Bengal, then over the SCS and ends over the Indian subcontinent. The relation among these three monsoon onsets, however, has strong interannual variability. For example, our results show that the Indian summer monsoon onset will occur earlier than the SCSSM onset and delay the SCSSM onset in SCSSM late onset years (Fig. 1). The year-to-year relationship and interaction among these three monsoons are not clear, and need further investigation.

Acknowledgements This work was supported by the China National 973 Project (2015CB453200), the National Natural Science Foundation of China (41420104002), the IPOVAR Project (GASI-IPOVAI-02), and the Natural Science Foundation of Jiangsu province (BK20150907). BW acknowledges supports from the NSF award #AGS-1540783, NOAA/DYNAMO # NA13OAR4310167 and the National Research Foundation (NRF) of Korea through a Global Research Laboratory (GRL) Grant (MEST, #2011–0021927). This paper is ESMC Contribution No. 195.

References

Chan JCL, Wang Y, Xu J (2000) Dynamic and thermodynamic characteristics associated with the onset of the 1998 South China Sea summer monsoon. J Meteorol Soc Jpn 78:367–380

Chang CP (1995) Tropical circulations associated with southwest monsoon onset and westerly surges over the South China Sea. Mon Weather Rev 123:3254–3267

Chen TC, Chen JM (1995) An Observational Study of the South China Sea monsoon during the 1979 summer: onset and life cycle. Mon Weather Rev 123:2295–2318

Dee D et al (2011) The ERA-Interim reanalysis: configuration and performance of the data assimilation system. Q J R Meteorol Soc 137:553–597

DeMott CA, Stan C, Randall DA (2013) Northward propagation mechanisms of the boreal summer intraseasonal oscillation in the ERA-Interim and SP-CCSM. J Clim 26:1973–1992

Ding YH (1992) Summer monsoon rainfalls in China. J Meteorol Soc Jpn 70:337–396

Ding Y, He C (2006) The summer monsoon onset over the tropical eastern Indian Ocean: the earliest onset process of the Asian summer monsoon. Adv Atmos Sci 23:940–950

Ding Y, Liu Y (2001) Onset and the evolution of the summer monsoon over the South China Sea during SCSMEX field experiment in 1998. J Meteorol Soc Jpn 79:255–276

Gao H, He J, Tan Y, Liu J (2001) Definition of 40-year onset date of south china sea summer monsoon. J Nanjing Inst Meteorol 24:379–383 **(in chinese)**

He J, Wen M, Wang L, Xu H (2006) Characteristics of the onset of the Asian summer monsoon and the importance of Asian-Australian "land bridge". Adv Atmos Sci 23:951–963

Huang RH, Sun FY (1992) Impacts of the tropical western Pacific on the East Asian summer monsoon. J Meteorol Soc Jpn 70:243–256

Jiang X, Li T, Wang B (2004) Structures and mechanisms of the northward propagating boreal summer intraseasonal oscillation. J Clim 17:1022–1039

Kajikawa Y, Wang B (2012) Interdecadal change of the South China Sea summer monsoon onset*. J Clim 25:3207–3218

Kajikawa Y, Yasunari T (2005) Interannual variability of the 10–25- and 30–60-day variation over the South China Sea during boreal summer. Geophys Res Lett 32:319–324

Kajikawa Y, Yasunari T, Wang B (2009) Decadal change in intraseasonal variability over the South China Sea. Geophys Res Lett 36:150–164

Kalnay E et al (1996) The NCEP/NCAR 40-Year Reanalysis Project. Bull Am Meteorol Soc 77:437–472

Kemball-cook S, Wang B (2001) Equatorial waves and air-sea interaction in the boreal summer intraseasonal oscillation. J Clim 14:2923–2942

Kueh M-T, Lin S-C (2009) A climatological study on the role of the South China Sea monsoon onset in the development of the East Asian summer monsoon. Theor Appl Climatol 99:163–186

Lau KM, Yang S (1997) Climatology and interannual variability of the Southeast Asian summer monsoon. Adv Atmos Sci 14:141–162

Lee J-Y, Wang B, Wheeler MC, Fu X, Waliser DE, Kang I-S (2013) Real-time multivariate indices for the boreal summer intraseasonal

oscillation over the Asian summer monsoon region. Clim Dyn 40:493–509
Li K, Yu W, Li T, Murty VSN, Khokiattiwong S, Adi TR, Budi S (2012) Structures and mechanisms of the first-branch northward-propagating intraseasonal oscillation over the tropical Indian Ocean. Clim Dyn 40:1707–1720
Li K, Li Z, Yang Y, Xiang B, Liu Y, Yu W (2015) Strong modulations on the Bay of Bengal monsoon onset vortex by the first northward-propagating intra-seasonal oscillation. Clim Dyn 47:107–115
Liang J, Wu S, You J (1999) The research on variations of onset time of the SCS summer monsoon and its intensity. J Trop Meteorol 15:97–105 **(in chinese)**
Liang JY, Wen ZP, Chen JP, Li-Ji Wu (2013) Characteristics of tropical sea surface temperature anomalies and their influences on the onset of South China Sea summer monsoon. Atmos Ocean Sci Lett 6:266–272
Liebmann B (1996) Description of a complete (interpolated) outgoing longwave radiation dataset. Bull Am Meteor Soc 77:1275–1277
Liu F, Wang B (2012) A conceptual model for self-sustained active-break Indian summer monsoon. Geophys Res Lett 39:611–625
Liu F, Wang B (2013) Mechanisms of global teleconnections associated with the asian summer monsoon: an intermediate model analysis*. J Clim 26:1791–1806
Liu Y, Chan JCL, Mao J, Wu G (2002) The Role of Bay of Bengal convection in the onset of the 1998 South China Sea summer monsoon. Mon Weather Rev 130:2731–2744
Liu X, Li Q, He J, Wang P (2010) Effects of the thermal contrast between Indo-China Peninsula and South China Sea on the SCS monsoon onset. J Meteorol Res 24:459–467 (chinese)
Liu B, Liu Y, Wu G, Yan J, He J, Ren S (2014) Asian summer monsoon onset barrier and its formation mechanism. Clim Dyn 45:711–726
Liu F, Wang B, Kang I-S (2015a) Roles of barotropic convective momentum transport in the intraseasonal oscillation*. J Clim 28:4908–4920
Liu F, Zhou L, Ling J, Fu X, Huang G (2015b) Relationship between SST anomalies and the intensity of intraseasonal variability. Theor Appl Climatol 124:847–854
Liu B, Zhu C, Yuan Y, Xu K (2016a) Two types of interannual variability of South China Sea summer monsoon onset related to the SST anomalies before and after 1993/94. J Clim 29:6957–6971
Liu F, Li T, Wang H, Deng L, Zhang Y (2016b) Modulation of boreal summer intraseasonal oscillations over the western North Pacific by ENSO. J Clim 29:7189–7201
Luo M, Leung Y, Graf H-F, Herzog M, Zhang W (2016) Interannual variability of the onset of the South China Sea summer monsoon. Int J Climatol 36:550–562
Madden RA, Julian PR (1971) Detection of a 40–50 day oscillation in the zonal wind in the tropical pacific. J Atmos Sci 28:702–708
Madden RA, Julian PR (1972) Description of global-scale circulation cells in the tropics with a 40–50 day period. J Atmos Sci 29:1109–1123
Mao J, Chan JCL (2005) Intraseasonal variability of the South China Sea summer monsoon. J Clim 18:2388–2402
Mao J, Wu G (2006) Interannual variability in the onset of the summer monsoon over the Eastern Bay of Bengal. Theor Appl Climatol 89:155–170
Mao J, Wu G (2008) Influences of Typhoon Chanchu on the 2006 South China Sea summer monsoon onset. Geophys Res Lett 35:82–90
Mao J, Chan JCL, Wu G (2004) Relationship between the onset of the South China Sea summer monsoon and the structure of the asian subtropical anticyclone. J Meteorol Soc Jpn 82:845–859
Murakami T, Matsumoto J (1994) Summer monsoon over the Asian continent and western North Pacific. J Meteorol Soc Jpn 72:719–745
Murakami T, Chen L, An X (1986) Relationships between seasonal cycles, low-frequency oscillations, and transient disturbances as revealed from outgoing longwave radiation data. Mon Weather Rev 114:1456–1465
Nitta T (1987) Convective activities in the tropical western Pacific and their impact on the northern hemisphere summer circulation. J Meteorol Soc Jpn 65:373–390
Shao X, Huang P, Huang R-H (2014) Role of the phase transition of intraseasonal oscillation on the South China Sea summer monsoon onset. Clim Dyn 45:125–137
Srinivasan J, Gadgil S, Webster PJ (1993) Meridional propagation of large-scale monsoon convective zones. Meteorol Atmos Phys 52:15–35
Straub KH, Kiladis GN, Ciesielski PE (2006) The role of equatorial waves in the onset of the South China Sea summer monsoon and the demise of El Niño during 1998. Dyn Atmos Oceans 42:216–238
Tong HW, Chan JCL, Zhou W (2008) The role of MJO and mid-latitude fronts in the South China Sea summer monsoon onset. Clim Dyn 33:827–841
Wang B (2002) Rainy Season of the Asian–Pacific summer monsoon*. J Clim 15:386–398
Wang B, LinHo (2002) Rainy season of the Asian–Pacific summer monsoon*. J Clim 15:386–398
Wang B, Xie X (1996) A model for the boreal summer intraseasonal oscillation. J Atmos Sci 54:72–86
Wang B, Xu X (1997) Northern hemisphere summer monsoon singularities and climatological intraseasonal oscillation. J Clim 10:1071–1085
Wang B, Zhang Y, Lu MM (2004) Definition of South China Sea monsoon onset and commencement of the East Asia summer monsoon. J Clim 17:699–710
Wang B, Ding Q, Joseph PV (2009a) Objective definition of the Indian summer monsoon onset*. J Clim 22:3303–3316
Wang B, Huang F, Wu Z, Yang J, Fu X, Kikuchi K (2009b) Multi-scale climate variability of the South China Sea monsoon: a review. Dyn Atmos Oceans 47:15–37
Webster PJ, Chou LC (1980) Low-frequency transitions of a simple monsoon system. J Atmos Sci 37:368–382
Webster PJ, Magaña VO, Palmer TN, Shukla J, Tomas RA, Yanai M, Yasunari T (1998) Monsoons: processes, predictability, and the prospects for prediction. J Geophys Res Atmos 1031:14451–14510
Wu R (2002) Processes for the northeastward advance of the summer monsoon over the western North Pacific. J Meteorol Soc Jpn 80:67–83
Wu R (2010) Subseasonal variability during the South China Sea summer monsoon onset. Clim Dyn 34:629–642
Wu R, Cao X (2017) Relationship of boreal summer 10–20-day and 30–60-day intraseasonal oscillation intensity over the tropical western North Pacific to tropical Indo-Pacific SST. Clim Dyn 48:3529–3546
Wu R, Wang B (2000) Interannual variability of summer monsoon onset over the western North Pacific and the underlying processes. J Clim 13:2483–2501
Wu R, Wang B (2001) Multi-stage onset of the summer monsoon over the western North Pacific. Clim Dyn 17:277–289
Xiang B, Wang B (2013) Mechanisms for the advanced Asian summer monsoon onset since the mid-to-late 1990s*. J Clim 26:1993–2009
Xie A, Chung YS, Liu X, Ye Q (1998) The interannual variations of the summer monsoon onset overthe South China Sea. Theor Appl Climatol 59:201–213
Yang J, Wang B, Wang B (2008) Anticorrelated intensity change of the quasi-biweekly and 30–50-day oscillations over the South China Sea. Geophys Res Lett 35:797–801
Yuan F, Chen W (2012) Roles of the tropical convective activities over different regions in the earlier onset of the South China Sea summer monsoon after 1993. Theor Appl Climatol 113:175–185

Yuan Y, Zhou W, Chan JCL, Li C (2008) Impacts of the basin-wide Indian Ocean SSTA on the South China Sea summer monsoon onset. Int J Climatol 28:1579–1587

Zhang C (2013) Madden–Julian oscillation: bridging weather and climate. Bull Am Meteorol Soc 94:1849–1870

Zhang Z, Chan JCL, Ding Y (2004) Characteristics, evolution and mechanisms of the summer monsoon onset over Southeast Asia. Int J Climatol 24:1461–1482

Zhou W, Chan JCL (2005) Intraseasonal oscillations and the South China Sea summer monsoon onset. Int J Climatol 25:1585–1609

Zhou W, Chan JCL (2007) ENSO and the South China Sea summer monsoon onset. Int J Climatol 27:157–167

Zhou L, Murtugudde R (2014) Impact of northward-propagating intraseasonal variability on the onset of indian summer monsoon. J Clim 27:126–139

Zhou T, Hsu H-H, Matsuno J (2011) Summer monsoons in East Asia, Indochina, and the western North Pacific. In: Chang C-P et al (eds) The Global Monsoon system: research and forecast, 2nd edn. World Scientific Publishing Co, Singapore, pp 43–72